Advances in Nano Research, *Vol. 9, No. 4 (2020) 263-276*
DOI: https://doi.org/10.12989/anr.2020.9.4.263

Acoustic responses of natural fibre reinforced nanocomposite structure using multiphysics approach and experimental validation

Rajesh Kumar Satankar[1a], Nitin Sharma[2b], Prashik Malhari Ramteke[1c], Subtra Kumar Panda[*1] and Siba Shankar Mahapatra[1d]

[1]*Department Mechanical Engineering, NIT Rourkela, Rourkela-769008, Sundergarh, Odisha, India*
[2]*School of Mechanical Engineering, KIIT Bhubaneswar, Bhubaneswar-751024, Odisha, India*

(*Received February 18, 2020, Revised September 22, 2020, Accepted September 25, 2020*)

Abstract. In this article, the acoustic responses of free vibrated natural fibre-reinforced polymer nanocomposite structure have been investigated first time with the help of commercial package (ANSYS) using the multiphysical modelling approach. The sound relevant data of the polymeric structure is obtained by varying weight fractions of the natural nanofibre within the composite. Firstly, the structural frequencies are obtained through a simulation model prepared in ANSYS and solved through the static structural analysis module. Further, the corresponding sound data within a certain range of frequencies are evaluated by modelling the medium through the boundary element steps with adequate coupling between structure and fluid via LMS Virtual Lab. The simulation model validity has been established by comparing the frequency and sound responses with published results. In addition, sets of experimentation are carried out for the eigenvalue and the sound pressure level for different weight fractions of natural fibre and compared with own simulation data. The experimental frequencies are obtained using own impact type vibration analyzer and recorded through LABVIEW support software. Similarly, the noise data due to the harmonically excited vibrating plate are recorded through the available Array microphone (40 PH and serial no: 190569). The numerical results and subsequent experimental comparison are indicating the comprehensiveness of the presently derived simulation model. Finally, the effects of structural design parameters (thickness ratio, aspect ratio and boundary conditions) on the acoustic behaviour of the natural-fibre reinforced nanocomposite are computed using the present multiphysical model and highlighted the inferences.

Keywords: layered composite; multiphysics (FE/BE) modelling; radiated sound power; experimental validation

1. Introduction

The current manufacturing industries are majorly adopting the low-cost material to improve the structural weight penalty considering not to hazard the environment. In this regard, the plant extracted fibres have been attracted the attention of the material scientist because of their adorable environmental friendly characteristics, which, in turn, includes the biodegradability as well as the low density (Arrakhiz *et al*. 2013, Belaadi *et al*. 2013, Joshi *et al*. 2004). Also, the surface characteristics of different plant extracted natural fibre have been evaluated by Sgriccia *et al*. (2008) to establish them as an alternative to the conventional material according to the present structural context. Further, it is a well-known fact that strength plays a major role in the application of the newly evolved fibres in the manufacturing field. Since last few decades, many of the researchers are exploring the capabilities of the natural fibre to be utilized in the load bearing components due to their well-known low strength in comparison to the synthetic fibre. In this regard, a number of innovative works are reported on natural plant fibre extracted bio-composites in the direction of improving the mechanical properties and to improve their strength for the high performing engineering field application. Also, the natural fibre has been utilized for few components of automotive/ marine/household cases (Béakou *et al*. 2008, Dayo *et al*. 2017), which are not sharing the major loading (parts of door panels, roof, marine field, and household appliances). However, luffa cylindrica is one of the natural fibre extracted from the fruit and available abundantly in the rural part of India. Moreover, the published research indicates that the major portion focuses on the mechanical characterization of luffa-fibre-reinforced polymer composite (Shen *et al*. 2012), acoustic properties (Koruk and Genc 2015) and their thermodynamic (Kong *et al*. 2017) behaviour. Anbukarasi and Kalaiselvam (2015) and Demir *et al*. (2006) are reported the enhancement of bonding between the fibre (luffa fibre) and matrix by alkali treatment. Further, its possible applications are increasing in the engineering industries like packaging, isolation of sound and vibration including impact energy absorption (Shen *et al*. 2012), too.

*Corresponding author, Associate Professor,
E-mail: pandask@nitrkl.ac.in; call2subrat@gmail.com
[a] Research Scholar, E-mail: satankarrajesh@gmail.com
[b] Associate Professor, E-mail: nits.iiit@gmail.com
[c] Research Scholar, E-mail: prashikramteke793@gmail.com
[d] Professor, E-mail: ssm@nitrkl.ac.in

ISSN: 2287-237X (Print), 2287-2388 (Online)

The natural fibre composite is light in weight and may also experience fatigue loading due to the vibrating environment. Therefore, it is necessary to investigate the frequency responses before their final structural application. In this regard, a selective review of available published research relevant to the frequency as well as the plant-fibre reinforced structure is discussed. The experimental (Kumar *et al*. 2014) free vibration characteristics of the hybrid polymeric composite structure are reported considering hybridization of two types of natural fibre i.e., sisal and banana fibre as well as other relevant design parameters (variation of length and percentage of fibre volume fraction). The free vibration frequency responses of the natural-fibre core-reinforced sandwich beam (Rajesh and Pitchaimani 2017) are reported considering glass fibre type of face sheets. The modal response measurement is mainly obtained to characterize the mechanical properties of fibre-reinforced composite materials and structures (Gibson 2000). Wang and Wang (2018) examined the frequency parameters of the bidirectional natural fibre reinforced composite under hygrothermal loading using the mechanical degradation model. Similarly, the free vibration characteristics of the pineapple leaf fibre-reinforced polyester composite are studied by Senthilkumar *et al*. (2019). The hybridization effect on the free vibration characteristics of the montmorillonite with coconut sheath/ polyester composite is examined experimentally by Rajini *et al*. (2013) via an impulse excitation technique. The FSDT kinematics has been adopted to investigate the vibrational frequency parameters of the anisotropic laminated composite (Ganapathi *et al*. 2009) structure. The FSDT kinematic model in association with moving least square differential quadrature technique has been adopted to predict the free vibration responses of the moderately thick symmetrically laminated composite plate (Liew 2003). Bert and Malik (1995) examined the effect of thickness shear deformation and rotary inertia on the free vibration frequencies of symmetric cross-ply laminated plate structure using a semi analytical differential quadrature technique. The free vibration characteristics of the cross-ply and antisymmetric angle-ply laminated plate analysed (Khdeir and Reddy 1999) using Levy type solution technique via the state space concept. Additionally, the higher-order refined kinematic theory utilized (Kant and Swaminathan 2001) to predict the frequency responses of the laminated and sandwich structures accurately.

Further, a list of the articles relevant to the sound pressure level is discussed for the synthetic and natural fibre composite structures considering the frequency range. In this regard, the enhancement of sound absorption characteristics of coir-fibre reinforced multilayer composite has been reported by Hosseini *et al*. (2010). Jayamani *et al*. (2016) found that the alkali treatment on natural fibre gives better sound absorption results as compared to untreated fibre. Berardi and Iannace (2015) investigated the sound absorption coefficient and flow resistance of natural fibre. Similarly, the absorption coefficient of treated and untreated luffa fibre examined by Jayamani *et al*. (2014). Also, Seddeq *et al*. (2012) investigated the sound absorption properties of recycled fibrous material. Putra *et al*. (2013), experimentally analyzed the sound-absorbing performance of sugarcane fibre. In addition, Prabhakaran *et al*. (2014) reported the sound absorption and damping properties of flax fibre. Erosy and Kucuk (2009) found that the sound absorption capacity of multilayer tea-leaf-fibre material was much higher than the equivalent number of woven textile cloth. The sound absorption coefficient increases with an increase in fibre content (Küçük and Korkmaz 2012).

In addition to the sound pressure level and frequency responses, some articles related to radiation efficiency of natural fibre reinforced composites are discussed here. The influence of different baffle angle and boundary conditions on the sound radiation efficiency of an isotropic rectangular plate investigated by Ohlrich and Hugin (2004) and Putra and Thompson (2010) whereas the same study has been performed by Atalla and Sgard (2015) for the baffled and unbaffled case. Also, the acoustic radiation behaviour of a plate under the distributed mass loading studied by Li and Li (2008). Acoustic radiated power has been investigated (Petrone *et al*. 2014) for the aluminum foam sandwich panel with different percentage of porosity.

Astley (1985) reported the mixed finite element method wave envelope scheme to account for the non-uniformity of subsonic means flow in the region of the vibrating structure. Peters *et al*. (2014) developed a model decomposition technique to analyse the individual modal contributions to the sound power radiation from an externally excited structure submerged in heavy fluid. Boundary element method has been developed (Ali *et al*. 1995, Meyer *et al*. 1978) using free-space Green's function and Helmholtz equation to find out the acoustic responses of the structure submerged in an infinite-extent fluid. Finite Element and Boundary Element (FE-BE) method used to determine the sound pressure field radiated by harmonically excited three-dimensional elastic structure (Everstine and Henderson 2013). FE-BE formulation has been developed (Junge *et al*. 2011) to solve the coupled eigenvalue problems between the structural domain and fluid domain interactions and obtained the corresponding acoustic responses as well. Jeyaraj (2010) investigated sound radiation characteristics of the isotropic square plate by utilizing FE-BE method. The acoustic response of the vibrating elliptical disc has been computed (Kumar *et al*. 2010) via FE-BE method (LMS SYSNOISE). The classical plate theory in association with LMS SYSNOISE has been used by Yin and Cui (2009) to compute the structural and acoustic response of laminated composite plate. The wave propagation method and Rayleigh-Ritz method employed by Park *et al*. (2003) to control the sound radiation and responses of the vibrating structure. A few articles relevant to theory, analysis, solution technique, kinematic model are already available in the published domain by a different group of researchers (Abualnour *et al*. 2019, Addou *et al*. 2019, Alimirzaei *et al*. 2019, Balubaid *et al*. 2019, Belbachir *et al*. 2019, Bousahla *et al*. 2020, Boussoula *et al*. 2020, Boutaleb *et al*. 2019, Draiche *et al*. 2019, Draoui *et al*. 2019, Kaddari *et al*. 2020, Karami *et al*. 2019a, b, 2020, Khiloun *et al*. 2020, Khosravi *et al*. 2020, Medani *et al*. 2019, Sahla *et al*. 2019, Tounsi *et al*. 2020) at different time. Also, the modelling and analysis of various structures presented (Abdul-Razza and Haido

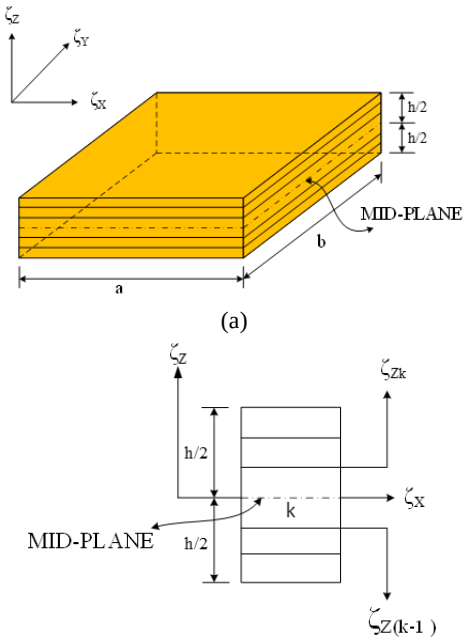

Fig. 1 Geometry of the natural fibre composite panel (a) laminated composite plate; (b) laminate configuration

2007, 2008, Abdul-Razzak and Mohammed Ali 2011, Alabduljabbar *et al*. 2020, Haido 2020, Shariati *et al*. 2020, Xu *et al*. 2019) by utilizing finite element method.

The present review indicates that the comprehensive volume of the research is already available to predict the acoustic characteristics of the laminated composite structure. Also, it can be seen that the sound-pressure data influenced by the variation in geometrical parameters (i.e., aspect ratio, thickness ratio) of the structure and their end support conditions. Similarly, the effort has already been made to investigate the sound absorption capabilities of natural/plant-fibre composite. But, it is found that no study relevant to the modelling and analysis of the structural acoustic responses of the natural fibre reinforced composite plate is available in the open literature. Therefore, in the present article, the authors investigated the vibroacoustic responses of luffa-fibre-reinforced composite structure very first time using a coupled FE-BE simulation model. Also, the model validation has been performed by comparing the simulation results with experimental and published data. In this regard, few luffa-fibre-reinforced composite plates have been prepared and the corresponding experiments are conducted to evaluate the elastic properties. Firstly, the natural frequency data of harmonically excited vibrating luffa-fibre-reinforced composite plate obtained by using the commercial FE package (ANSYS). Further, the acoustic responses are obtained for the free vibrated structure by utilizing indirect BE method in the LMS virtual environment. Finally, the model has been extended to investigate the effect of different design parameters (i.e., aspect ratio, thickness ratio, support conditions) on the acoustic radiation characteristics of an un-baffled composite plate and the details are highlighted for the future reference.

2. Theoretical formulation

For the present acoustic analysis, a physical model of fruit extracted fibre (luffa cylidrcia) reinforced composite has been derived mathematically considering the related geometrical dimension (length, width and thickness as 'a', 'b' and 'h', respectively) and provided in Fig. 1. The deformation behaviour of the structural component has been expressed with the help of first-order shear deformation kinematic model including the moderate shear deformation and the thickness stretching effect.

The composite plate modelled using static structural analysis module of ANSYS using the batch input technique (APDL code). The mathematical model of the composite has been expressed considering the six degrees of freedom per node and conceded as

$$\begin{aligned}\overline{U}\{\zeta_x,\zeta_y,\zeta_z,T\} &= \overline{U}_0\{\zeta_x,\zeta_y\} + \bar{Z}\phi_x\{\zeta_x,\zeta_y\}\\ \overline{V}\{\zeta_x,\zeta_y,\zeta_z,T\} &= \overline{V}_0\{\zeta_x,\zeta_y\} + \bar{Z}\phi_y\{\zeta_x,\zeta_y\}\\ \overline{W}\{\zeta_x,\zeta_y,\zeta_z,T\} &= \overline{W}_0\{\zeta_x,\zeta_y\} + \bar{Z}\phi_z\{\zeta_x,\zeta_y\}\end{aligned} \quad (1)$$

where, $\overline{U}$, $\overline{V}$ and $\overline{W}$ represent the displacement at a point on the mid-layer (k^{th} layer) of the surface of the lamina along the ζ_x, ζ_y and ζ_z coordinate axes, at the time "T". Whereas $\overline{U}_0$, $\overline{V}_0$ and $\overline{W}_0$ are representing the displacements of a point on the mid-plane, ϕ_x and ϕ_y denote the rotations of normal to the mid-surface (ζ_z = 0) along the ζ_y and ζ_x respectively, ϕ_z is the higher-order term in the Taylor series expansion which accounts for the linear variation of displacement function along the thickness direction.

Further, to determine the modal values of the structure are obtained using the Block Lanczos technique from the simulation tool. The modes of the vibrating structure have been found out by solving the given eigenvalue equation (Cook *et al*. 2000).

$$([K]-\omega^2[M])\{\Phi\}=0 \quad (2)$$

where [K] stand for the stiffness and [M] stand for the mass, whereas ω and $\{\Phi\}$ represents the natural frequency of vibration, mode shape vector respectively. Now, extract the values of mode shape from the computed natural frequencies.

Similar to the finite element technique, BEM is highly recommended for the solution of the coupled vibroacoustic problem. The indirect BEM method has been utilized to evaluate the acoustic responses of the structure with the un-baffled condition in the fluid medium. The Helmholtz equation for the wave propagation is considered to solve the acoustic responses of the composite structure under the fluid medium (D) and expressed as

$$\nabla^2 p' + k^2 p' = 0 \text{ and } k = \omega/c \quad (3)$$

where ∇^2 is the Laplacian symbol whereas k, p', ω and c representing the wavenumber, acoustic pressure, angular frequency and the speed of sound, respectively in the surrounding acoustic medium (D). Additionally, S^+ and S^- are denoting both sides of the surface S separately, such that

$s = s^+ \cup s^-$.

The indirect BEM method considers for the modelling of acoustic variables in the form of potentials, in which, σ represent the single-layer potential and μ double-layer potential. These potentials are related to the acoustic pressure and velocity jumps across the surface *S* as

$$\sigma = \frac{\partial p'^{+}}{\partial n} - \frac{\partial p'^{-}}{\partial n} \tag{4}$$

and

$$\mu = p'^{+} - p'^{-} \tag{5}$$

where superscripts '+' represent the value on the positive side, it is outward normal vector on the surface, s^+ and the superscripts '−' represents the value on the opposite side, i.e., s^-. After introducing the potential (Eq. (5)) into the Helmholtz wave equation and takes to another form as in the source (Nowak and Zielinski 2015)

$$p^{'} = -\int_s \left[G_{xy}^{'} \sigma_y - \frac{\partial G_{xy}^{'}}{\partial n_y} \mu_y \right] dS_y, \quad \forall x \notin S \text{ and } y \in S \tag{6}$$

where *G* represents the Green's function and can be defined as

$$G'_{xy} = \frac{1}{4\pi r} e^{-jkr} \tag{7}$$

where *r* represents the distance between the point of source y and point on the field *x*.

Now, apply the Neumann's boundary relation to solve the Eq. (3) for vibrating plate which is expressed as

$$\sigma = 0 \quad \text{and} \quad \left.\frac{\partial p^{'}}{\partial n}\right|_y = -jw\rho V_n \quad \text{for} \quad y \in S \tag{8}$$

where V_n represent the normal component of the velocity of the structure. The above equation can be re-written as follows by applying the boundary condition as follows.

$$-j\omega\rho V_n = \int_s \mu_y \frac{\partial^2 G_{xy}}{\partial n_x \partial n_y} dS_y \tag{9}$$

Also, the value of potential μ can be obtained by solving the earlier equation and minimizing the functional *J* and expressed as

$$J = 2\int_s j\omega\rho\mu_x V_{n,y} + \int_s \int_s \mu_x \mu_y \frac{\partial^2 G'_{xy}}{\partial n_x \partial n_y} dS_x dS_y \tag{10}$$

Eq. (10) is another form of equation got through using Green's function *G* and potential μ (Tournour and Atalla 1998)

$$\left.\begin{aligned} \int_s \int_s \mu_x \mu_y \frac{\partial^2 G'_{xy}}{\partial n_x \partial n_y} dS_x dS_y = \\ \int_s \int_s G'_{xy} \left[k^2 \mu_x \mu_y (n_x . n_y) - (\nabla \times \mu_x).(\nabla \times \mu_y) \right] dS_x dS_y \\ = \langle \mu \rangle [D(\omega)] \{\mu\} \end{aligned}\right\} \tag{11}$$

and

$$\int_s j\omega\rho\mu_x V_{n,y} = \langle U \rangle [C] \{\mu\} \tag{12}$$

where *U* represent d.o.f (degrees of freedom vector) of the structure. Therefore, a coupling between the structure and the acoustic is mentioned using the matrix representation as

$$\begin{bmatrix} K + i\omega\Theta - \omega^2 M & C \\ C^T & -\frac{1}{\rho\omega^2} D(\omega) \end{bmatrix} \begin{Bmatrix} U \\ \mu \end{Bmatrix} = \begin{Bmatrix} F \\ 0 \end{Bmatrix} \tag{13}$$

where Θ represents damping matrix and *F* is the external load vector. The system is symmetric, frequency-dependent and full. Now, Eq. (13) is solved to compute the values of *U* and μ.

Further, the impedance matrix of the radiated sound power as mentioned below considering the steps from the source (Atalla and Sgard 2015)

$$Z(\omega) = -j\rho\omega C D(\omega)^{-1} C^T \tag{14}$$

The radiated power of the sound (W_{rad}) of the vibrating plate as given below (Atalla and Sgard 2015)

$$W_{rad} = \frac{\omega^2}{2} \langle U^* \rangle real[Z(\omega)] \{U\} \tag{15}$$

The radiated sound power level is expressed as

$$\text{Sound Power Level} = 10 \times \log\left(\frac{W_{rad}}{W_{ref}}\right) \tag{16}$$

where W_{ref} is the reference power and in the present analysis, it is taken to be equal to 10^{-12} W.

3. Methodology

According to the theory, it is clear that developed the model in FEM for a structural response then coupled it with a Boundary Element Method (BEM) by LMS sysnoise software for obtained the acoustic responses.

The following steps are considered to find out the vibroacoustic solution of the lamina structure panel:

I. The ANSYS with APDL code, using FSDT theory to develop the structural model of lamina flat panel. For the discretization, the structure, consider shell 281 iso-parametric element.

II. The mode shapes and natural frequency are found after apply the support condition on the modal. The support condition as discussed below.

(a) All boundaries are clamped condition (CCCC): $\overline{U}_0 = \overline{V}_0 = \overline{W}_0 = \phi_x = \phi_y = \phi_z = 0$ at $x = 0$ and a; $y = 0$ and b.

(b) One edge clamped and others free: $\overline{U}_0 = \overline{V}_0 = \overline{W}_0 = \phi_x = \phi_y = \phi_z = 0$ at $x = 0$ only.

III. The mechanical properties and end condition of the lamina flat panel structure contained in the ANSYS file (.rst extension).

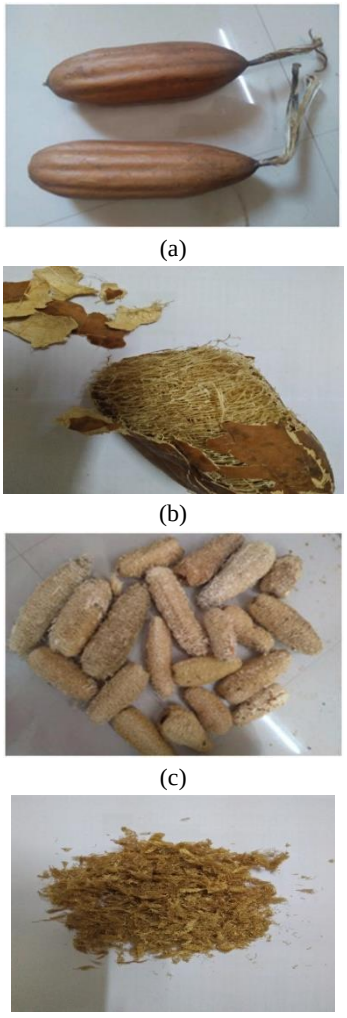

(a) (b) (c) (d)

Fig. 2 Processing of luffa fibre preparation (a) dry form; (b) uncovered form of luffa cylindrica; (c) untreated luffa cylindrica; (d) chopped form of treated luffa

IV. All the data from ANSYS file (.rst file) imported into LMS Virtual Lab environment for computing the acoustic responses.

Acoustic simulation via LMS Virtual. Lab acoustic helps to predict the sound and noise performance of the lamina composite panel.

(a) Firstly, import the ANSYS file (.rst file) imported into LMS Virtual Lab environment browse the structural.rst and acoustic.rst file.

(b) To set the mesh part type for this select the set as structural and acoustical as concerning structural and acoustic (.rst) file.

(c) Structural and acoustical mesh part contained the identical nodes and element due to this can lead the conflict to avoid the numbering conflict check the ID conflicts and fix the element id conflicts between the two mesh parts.

(d) Insert the properties as new fluid property to apply the fluid property to the acoustical mesh part and create the manual mesh group.

(e) Import file data from the ANSYS (.rst) for analyzing the dynamic behaviour of structural select the vector function and function creator for import the load file through this imported the corresponding frequencies and harmonic load.

(f) Execute the coupled vibroacoustic analysis of the model created through modal superposition vibroacoustic response analysis.

(g) Finally, the results are displayed and get the radiated sound power then result are exported for further analysis.

The present numerical results compared with experimental results for the authentication of computed simulation data.

Table 1 Set of a composite at varying weight of fraction of fibre

Composite	C_1	C_2	C_3	C_4
Weight of fibre (gm)	0	14.72	29.44	44.16
Weight of epoxy (gm)	460	445.28	430.56	415.84
Fibre weight fraction (%)	0	3.2	6.4	9.6

4. Fibre extraction, treatment and composite preparation

Luffa cylindrica is a kind of vegetable, which is available abundantly in the villages of India, most of the people used it as a vegetable. Luffa fibre gets the cylindrical form after it ripped and dry as shown in Fig. 2(a). Then the outer cover has been removed as shown in Fig. 2(b) and fibres are presented in the form of the net inside the luffa. These luffa fibres have gums and impurities within it. Therefore, it is necessary to remove these impurities from the fibre to achieve better adhesion between the fibre and matrix. In this regard, many researchers show how to improve the bonding properties between the fibre and matrix by treatment of luffa fibre with NaOH solution. The similar process is used in this article as well for the improvement of bonding properties. In this regard, the fibre washed first by tap water and then with the distilled water for the removal of dirt. The washed fibres are then dried at the ambient temperature. Demir *et al*. (2006) investigated that the improved surface roughness leads to better mechanical bonding with the matrix. They soaked the fibre into 5% NaOH for 4 hours. Subsequently, the treated fibre washed properly by distilled water and left to dry it in the sunlight for 3-4 hours. The treated dried fibre then chopped into the small pieces (2-5 mm) for the preparation of a natural fibre-reinforced composite.

In fabrication process, a thermoset polymer resin (Lapox L-12) is used as a matrix material along with the hardener (K-6). This matrix is not a biodegradable type of matrix and well known in the field of composite manufacturing because of excellent properties. Initially, a mould (270 mm × 270 mm × 5 mm) is prepared using the wooden strips. Then the treated form of luffa fibres added into the epoxy resin and this mixture is then filled into the mould and left for 72 hours for the curing process. This process is repeated for the fabrication of different type of composite plates with

Table 2 Elastic properties of fabricated composite

Composite	C_1	C_2	C_3	C_4
Density (g/cm^3)	1.1501	1.1377	1.1258	1.1142
Young's modulus (GPa)	4.27	4.71	4.95	5.56

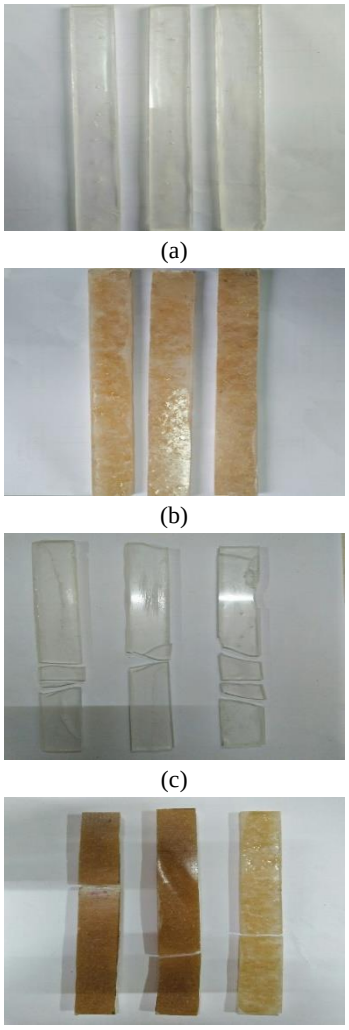

(a) (b) (c) (d)

Fig. 3 Test specimen for tensile test (a) pure epoxy (before test); (b) with fibre content (before test); (c) pure epoxy (after test); (d) with fibre content (after test)

different weight fractions of luffa fibre i.e., 0%, 3.2%, 6.4% and 9.6% and the details are given in Table 1. The fabricated composite plates labelled the name as pure epoxy plate (C_1), plate with 3.2% of luffa (C_2), plate with 6.4% of luffa (C_3) and plate with 9.6% of luffa (C_4).

5. An experiment test for the evaluation of material properties (density and Young's modulus)

The simple water immersion technique is used for the calculation of densities of the samples. For this purpose, five different samples are prepared for the calculation of densities. The samples are cut from the different position of the fabricated plates. Table 2 shows the average density of each set of the composite. It is observed from the table that the mass density of the composite plate follows the declined trend with increase in the fibre volume fraction as it has low specific weight.

For evaluating the elastic properties of the composite, the test specimen prepared according to ASTM standard (D3039) as presented in Figs. 3(a)-(b). The test is performed on the Universal Testing Machine (UTM) INSTRON-1195 that is available in the parent institute at Rourkela, India. The five-test samples have been tested for each type of composite and the average value is considered for evaluating the Young's modulus of the composite. The test specimen C_1 has least value while the highest value of the Young's modulus is obtained for sample C_4.

Table 3 Convergence and validation of natural frequencies under the clamped condition

Mesh size	Mode 1	Mode 2	Mode 3	Mode 4	Mode 5
2 × 2	250.3698	499.2159	499.1236	728.9630	951.2369
4 × 4	240.1236	493.1256	493.1145	725.1258	947.1258
6 × 6	232.3922	492.3979	492.3979	724.1238	946.8060
8 × 8	227.0942	469.5328	469.5328	689.4740	863.5878
9 × 9	225.8255	464.2790	464.2790	681.5610	845.4378
10 × 10	224.9817	460.8296	460.8296	676.3670	833.7195
12 × 12	223.9927	456.8323	456.8323	670.3388	820.3342
14 × 14	223.9724	456.8319	456.8329	670.3350	820.3341
Jeyaraj (2010)	224	456	456	673	819

6. Result and discussion

The vibration under the free condition and sound responses of the lamina composite plate is computed by the proposed scheme (ANSYS for structural responses followed by LMS Virtual Lab for acoustic responses). The convergence test and subsequent validation have been established by available open literature, and the numerical results are compared with the experimental results to check the accuracy of the proposed scheme. The effect of various parameters, thickness ratio (a/h), aspect ratio (a/b), on the acoustic response of proposed lamina flat panel by using different boundary conditions (CCCC, CFCF, CCCF and CFFF) have been investigated. The panel of the structure is considered to be excited by 1 N harmonic load applied on the surface at a central location. A modal damping 1% has been considered for the analysis.

6.1 Validation study

6.1.1 Convergence and validation of frequency responses

The convergence and validation test performed by solving the problem of the isotropic plate for both vibration response and acoustic behaviour of the present model. For

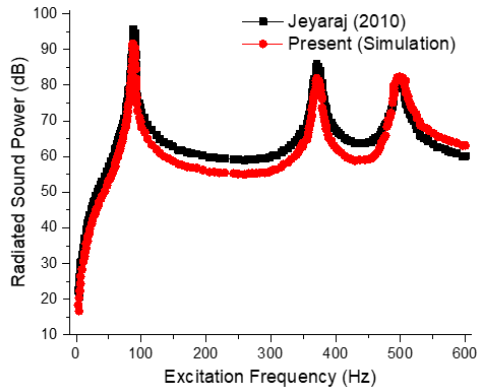

Fig. 4 Validation of acoustic response

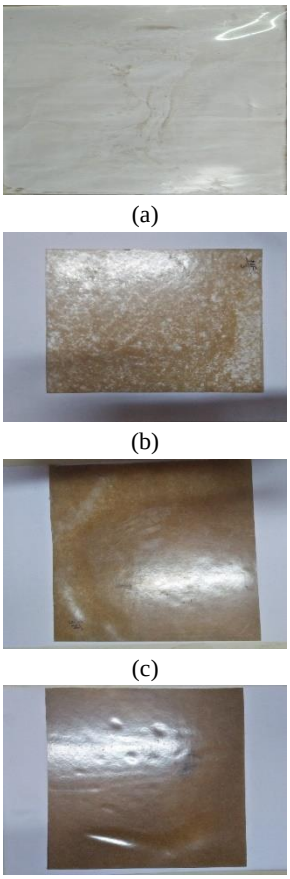

(a) (b) (c) (d)

Fig. 5 Test specimen for acoustic test (a) neat epoxy; (b) 3.2 % fibre content; (c) 6.4 % fibre; (d) 9.6 % fibre content

this purpose, the frequency responses are obtained by using a square clamped isotropic (mild-steel) plate consider the same geometrical and material parameters as Jeyaraj (2010) and presented in Table 3. It is evident from the results that the responses converging well with the mesh refinement. In addition, the results are compared with the available published literature for different mode number. Based on the convergence test of model a (12 × 12) has been employed for computing the responses for further analysis of the model.

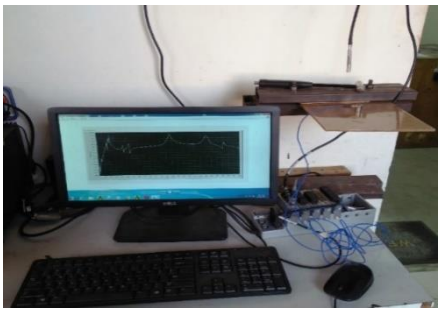

(a)

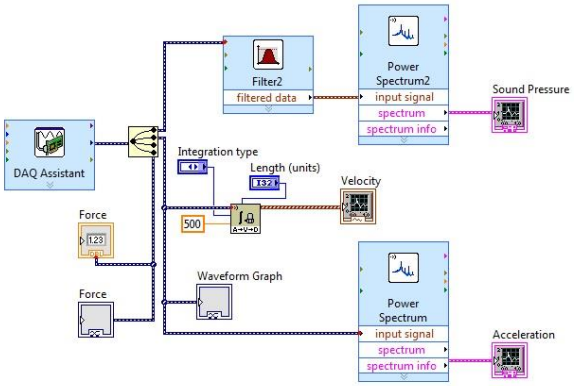

(b)

Fig. 6 (a) Experimental set-up for measuring natural frequencies and SPL under cantilever condition: (1) luffa fibre lamina plate (2) fixture (3) impact hammer (4) accelerometer (5) microphone (6) NI PXI e 1071; (b) circuit diagram of LABVIEW to record vibration and acoustic response of lamina flat panel

6.1.2 Numerical validation of vibroacoustic responses

The validation test has been performed to check the accuracy of the acoustic responses of the present model. In order to do so, the example is considered as given in Jeyaraj (2010) for the rectangular isotropic plate (a = 0.455 m, b = 0.379 m, h = 0.003 m, E = 2.1 × 10^{11} N/m^2, ν = 0.3, ρ = 7850 kg/m^3) subjected to harmonic point load of 1 N at the plate centre. The radiated sound power level from the vibrating plate has been obtained by using the present FE-BE (ANSYS and LMS Virtual Lab) scheme. Now compare the responses obtained through the present scheme with reference data as shown in Fig. 4. It can be seen from Fig. 4 that the responses obtained through the present model are in good agreement with reference data.

6.1.3 Experimental validation for frequency responses

Vibration test is performed by using vibration apparatus cDAQ-9178 (compact data acquisition). The test specimen size 0.18 m × 0.18 m × 0.005 m are prepared (as mentioned in the manual) with varying content of fibre according to Table 1 (fabricated specimen as shown in Fig. 5). To perform the test, the plate is fixed on the fixture according to one side fixed and others are free (CFFF). The electronic hammer is used for the initial excitement on the surface of the plate. Therefore, acceleration is generated in analogue

Table 4 Comparison of experimental and simulation data for the frequency responses of the first three modes

Composite of different weight fraction of luffa fibre		Natural frequency (Hz)		
		Mode 1	Mode 2	Mode 3
C_1	Simulation	49.909	122.089	311.115
	Experimental	48.128	123.659	259.7624
C_2	Simulation	52.708	128.956	328.614
	Experimental	50.281	124.355	303.823
C_3	Simulation	54.321	132.904	338.671
	Experimental	52.379	128.062	315.468
C_4	Simulation	57.855	141.548	360.704
	Experimental	55.488	125.208	325.108

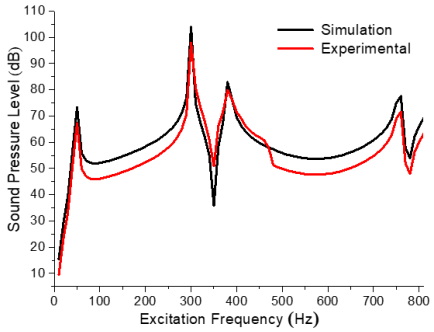

Fig. 7 Experimental validation of sound pressure level for the vibrating plate structure of luffa fibre composite

form via accelerometer (352C03). The analogue signal converted into the digital signals via cDAQ-9178 (compact data acquisition). Then these signals further processed through Lab View Virtual program (as shown in Fig. 6) and the final frequency response is obtained. This experimental response is compared with the numerical results, it shows good agreement with numerical results, which is presented in Table 4.

It is clearly seen from Table 4 that the value of natural frequency at all considered modes increases with various weight fraction of composites. The experimental values are slightly lower than the numerical values. It is due to the difficulty in achieving the perfect boundary condition. As per table data indicate the increasing trend of the responses with the composite C_1, C_2, C_3 and C_4. This is due to increasing Young's modulus.

6.1.4 Experimental validation of sound pressure level

Lamina of higher weight fraction of fibre (C_4) considered for computing the responses of Sound Pressure Level (SPL) at a point on the plate under the CFFF boundary conditions. The plate is excited by the 1 N of harmonic load at the centre node of the surface for vibrating the structure. The vibration is generated after the excitement of the structure and measured the corresponding sound pressure level approximate 1 m distance above the exciting point of the plate. For computing, the SPL of the plate

Table 5 Structural parameters for analysis

Parameters	Variation
Thickness ratio	$a = b = 0.18$ m h varies according to thickness ratio (a/h)
Aspect ratio	$a = 0.18$ m, $h = 0.005$ m b varies according to aspect ratio (a/b)

Table 6 Coincidence frequency of different composite according to thickness ratio (a/h)

Composite type	Coincidence frequency $\left(=\frac{c^2}{2\pi h}\sqrt{\frac{12\rho(1-\nu^2)}{E}}\right)$					
	Thickness ratio (a/h)					
	10	20	30	50	80	100
C_1	180.481	360.962	541.443	902.406	1443.850	1804.812
C_2	170.870	341.740	512.611	854.352	1366.963	1708.704
C_3	165.794	331.589	497.384	828.973	1193.722	1657.947
C_4	155.669	311.338	467.007	778.345	1120.817	1556.690

numerically considered similar test conditions as mentioned in the experimental test. Comparison between the experimental and numerical results of SPL of the vibrating plate as shown in Fig. 7. It observed that the experimental result of SPL follows closely with the numerical result up to the excitation frequency of 300 Hz.

6.2 New illustrations

After the necessary sensitivity and validation of the proposed simulation model, it has been extended to show the effect of individual and/or combined parametric effect on the sound characteristics. In this regard, a series of numerical examples are solved by varying different geometrical parameter and their effects are presented in the following subsections. The results are obtained for all four kinds of fabricated composite panel i.e., C_1, C_2, C3 and C_4, if not stated otherwise. Additionally, the geometrical parameters and their variations for the current analysis are shown in Table 5.

6.2.1 Influence of thickness ratio

Firstly, the effect of variable structural thickness parameter (a/h = 10, 20, 30, 50, 80 and 100) on the composite structural panel sound level has been computed using the proposed simulation model. In addition, the responses are calculated considering with and without fibre within the composite i.e., pure epoxy and different weight fraction of luffa. The variation of structural thickness is achieved by considering the variable 'h' and constant 'a' the corresponding value of the side taken as according to the size mentioned in Table 5. The sound power has been computed by considering the coincidence frequency of each type of composite plate (C_1, C_2, C_3 and C_4). It can be clearly understood from the mathematical expression of coincidence frequency that it depends on the three major parameters (component thickness, density and Young's

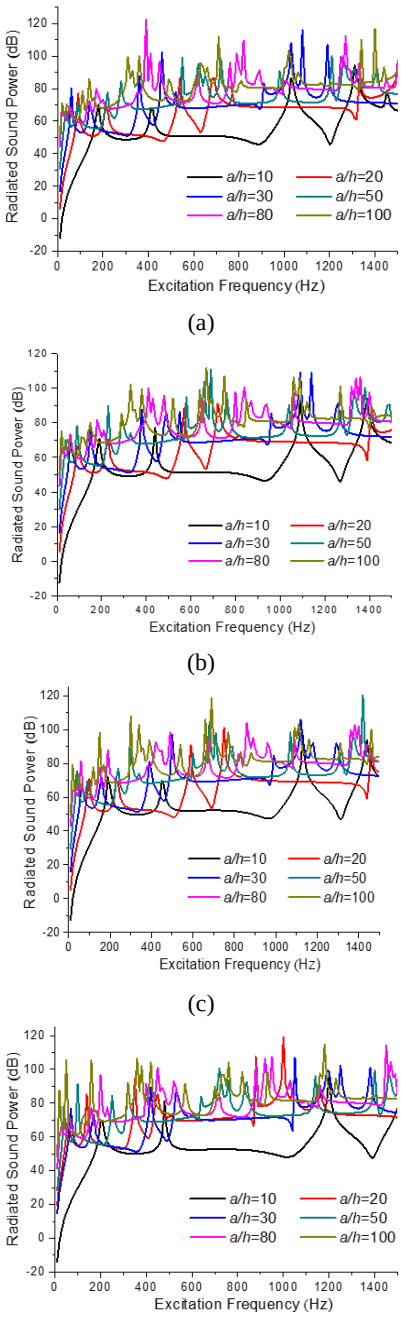

Fig. 8 Effect of thickness ratio on radiated acoustic power of four different weight fraction of luffa fibre composite (a) composite C_1; (b) composite C_2; (c) composite C_3; (d) composite C_4

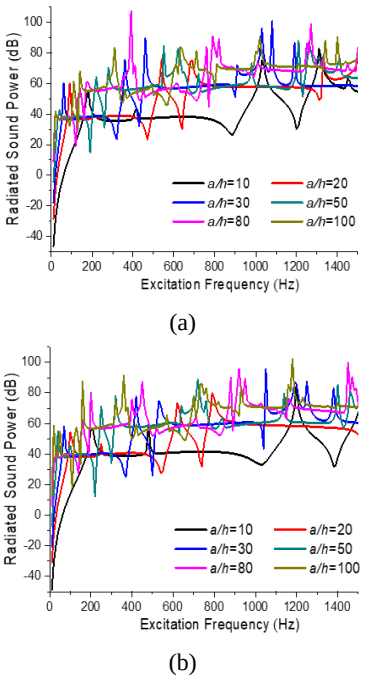

Fig. 9 Effect of thickness ratio on sound pressure level of two different weight fraction of luffa fibre composite (a) composite C_1; (b) composite C_4

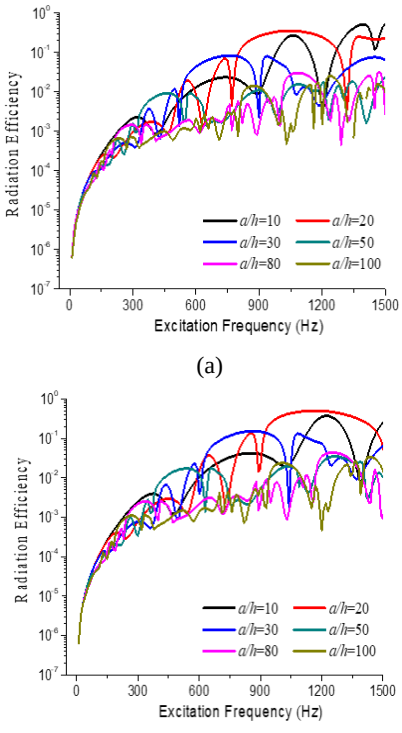

Fig. 10 Effect of thickness ratio on radiation efficiency of two different weight fraction of luffa fibre composite: (a) composite C_1; (b) composite C_4

modulus). Since each plate has different elastic strength and the thickness, hence, the coincidence frequency values also vary accordingly. This is because of four types of composite component utilized in the current analysis-containing no or maximum weight fractions luffa fibre. The coincidence frequencies (Hz) for each type of composite including their thickness parameters can be seen in Table 6. It can be observed from the tabular data that the maximum value of the frequency is < 1900, hence, 0-2000 Hz range has been adopted for the current analysis. Also, the coincidence frequency values are following a decreasing line when thickness ratio values are increasing for composite C_1 to C_4 and the responses follow the expected line as per the

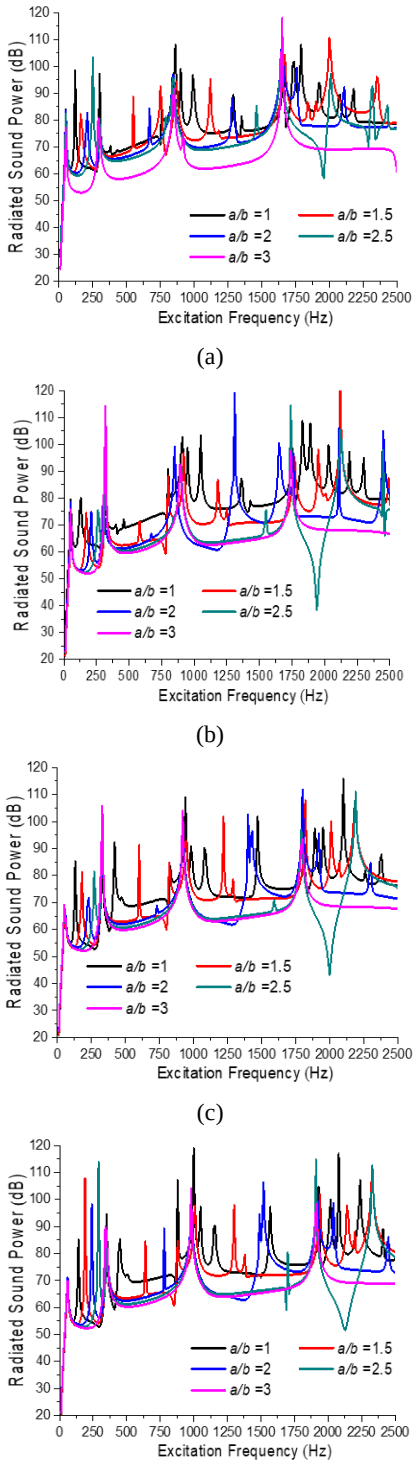

Fig. 11 Effect of aspect ratio on radiated acoustic power of four different weight fraction of luffa fibre composite (a) composite C_1; (b) composite C_2; (c) composite C_3; (d) composite C_4

mathematical expression. This is because the composite density is decreasing and elastic modulus (Table 2) increasing when the luffa fraction increases. Figs. 8(a)-(d) are showing the variation of the radiated sound power for all four fabricated composite plates (C_1, C_2, C_3 and C_4)

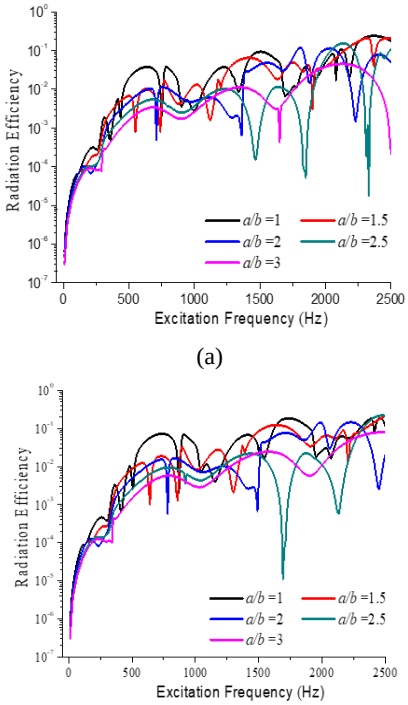

Fig. 12 Effect of aspect ratio on radiation efficiency of two different weight fraction of luffa fibre composite (a) composite C_1; (b) composite C_4

along with the numerical excitation frequency value. It is worthy to note that the radiated sound power values are increased when the thickness ratio of the panel increases. This is because of the reduction in stiffness values of the thin structural components while the thickness ratio increase.

Further, the sound pressure level data are plotted in Fig. 9 considering the input parameters as same as the earlier example. The pressure level is obtained for two kinds of composite panels i.e., C_1 (not containing luffa fibre) and C_4 (have highest contained luffa fibre). It is observed that the sound pressure level is increasing with the higher thickness ratios (reduction of total stiffness of thin structural component). Additionally, the sound radiation efficiency of the composite C_1 and C_4 are shown in Figs. 10(a) and (b). The graph is following the similar trend as in the case of sound-power and sound-pressure case i.e., the radiation efficiency decreases while thickness parameter increases for C_1 and C_4 composites. The distinct variations are not observed due to the multiple mode interaction. The obtained results are indicating the effect of plant fibre effect on the sound radiation efficiency of the natural fibre.

6.2.2 Influence of aspect ratio

In this example, the influences of different aspect ratios (a/b = 1, 1.5, 2, 2.5 and 3) on the radiated sound power and sound radiation efficiency are computed using the current simulation model. The sound-related data and the corresponding frequency parameters are obtained on the in-house fabricated natural fibre-reinforced composite (a = 0.18 m and h = 0.005 m). The responses are computed for

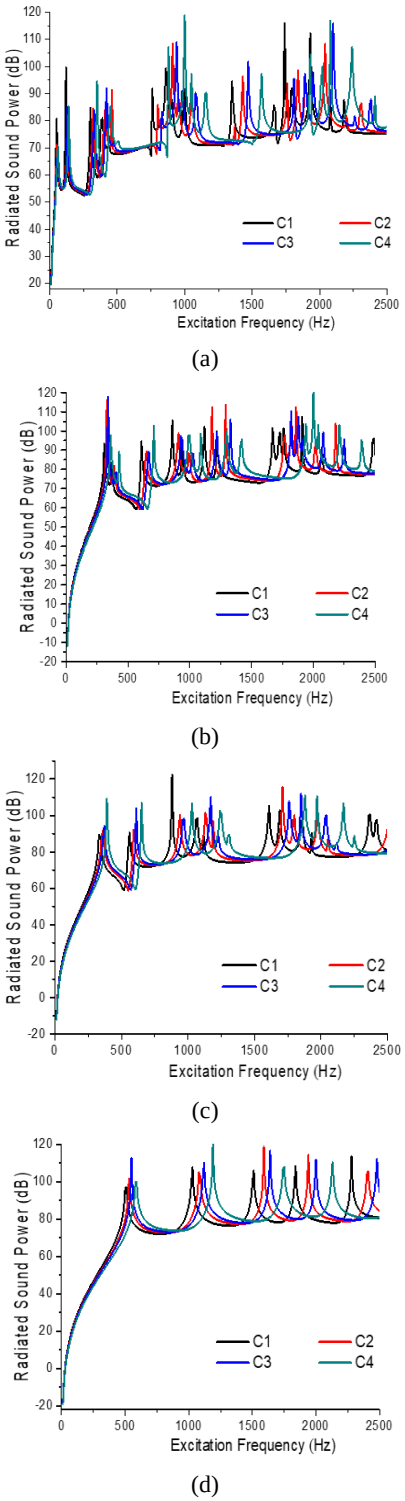

Fig. 13 Effect of boundary condition on radiated acoustic power of four different weight fraction of luffa fibre composite (a) CFFF; (b) CFCF; (c) CCCF; (d) CCCC

all kinds of fabricated composite (C_1, C_2, C_3 and C_4) by varying the luffa sponge extract. Moreover, the radiated sound-power data are computed by extracting the coincidence frequencies (Hz) for the different composite plate are 649.732, 615.135, 619.825 and 560.408 for each case i.e., C_1, C_2, C_3 and C_4, respectively. It is clear from the sound power response and the radiation efficiency i.e., Figs. 11(a)-(d) and Figs. 12(a)-(b), respectively, follow an increasing path when the aspect ratio values decrease for all four in-house fabricated composite components (epoxy and luffa-fibre-reinforced structure).

6.2.3 Influence of boundary condition

The end support conditions are playing a significant role in the structural stiffness since the number of constraints modifies the total structural stiffness. The stiffness of the structure is increasing while the number of constraints increases. Therefore, the sound power responses are decreasing with the increased number of end boundary constraint. It is clearly seen from Figs. 13(a)-(d) that the boundary conditions (CFFF, CFCF, CCCF and CCCC) are influencing the corresponding sound power responses of the luffa-fibre-reinforced epoxy composite (C_1, C_2, C_3 and C_4). The acoustic responses are simulated by changing the number of constraints from free to clamped for each case i.e., Figs. 13(a)-(d), where the free boundaries are converted clamped. Due to the increase in the number of constraints the structural component becomes stiff and the subsequent sound data become low. Hence, the results follow the anticipated trend for different end boundary cases.

7. Conclusions

This research article reported the eigenfrequency data and their acoustic responses of fruit extracted luffa fibre-reinforced composite using a coupling type simulation model. The fibre within the composite is considered to be distributed randomly and the properties similar to the isotropic material. The frequency and the sound-related responses are simulated using the ANSYS APDL code in association with the LMS virtual lab. Moreover, four composite plates are fabricated using the different weight fractions of the fibre for the experimental purpose. The prepared simulation model validity has been verified in two steps i.e., comparing with published simulation results and in-house experimentation including the experimental properties (neat epoxy and luffa-reinforced/epoxy). Further, sets of numerical examples are solved to evaluate three major output for the sound relevant study i.e., radiated sound-power, sound-pressure level and sound-radiation efficiency. The results are computed by considering the variation of geometrical parameter (aspect ratio, thickness ratio and end constraint conditions) as well as the fibre contained.

- The radiated acoustic power, sound pressure and radiation efficiency increased with an increase in the thickness ratio. It is due to the fact that the stiffness of composite decreases with increasing thickness ratio.
- It is also observed that the variation of weight fractions of fibre contained in the composite influences the sound responses considerably because of the absorbing capacity of luffa present in the composite. Hence, the radiation of the sound responses is following a decremental path with the increasing weight fraction of fibre.

• Similarly, the computed results for the different aspect ratios also follow the anticipated line i.e., the sound-power decreases with increasing aspect ratio. It can also be observed that the efficiency data is insignificant for the change in volume fraction in comparison to the aspect ratio. This is mainly due to the lower volume fractions of fibre contained within the composite and increasing in volume fraction needs meticulousness to avoid the agglomeration and smooth mixing.

• Moreover, the analysis relevant to the support conditions is providing the meaningful insight i.e., the sound relevant data affected due to the change in structural stiffness. The acoustic power radiated showing higher for cantilever (CFFF) structure whereas lower for the CCCC boundaries. The numbers of end constraint are increasing from the CFFF to CCCC boundary conditions and the radiating responses vary accordingly.

Acknowledgments

The authors of the article are thankful to Prof. M. Rajesh, Department of Design and Automation, School of Mechanical Engineering, VIT University, Vellore 632014, TN, India for providing access to LMS Virtual. Lab.

References

Abdul-Razzak, A.A. and Haido, J.H. (2007), "Free vibration analysis of rectangular plates using higher order finite layer method", *AL-Rafidain Eng. J.*, **15**(3), 19-32.

Abdul-Razzak, A.A. and Haido, J.H. (2008), "Forced vibration analysis of rectagular plates using higher order finite layer method", *AL-Rafidain Eng. J.*, **16**(5), 43-56.

Abdul-Razzak, A.A. and Mohammed Ali, A.A. (2011), "Influence of cracked concrete models on the nonlinear analysis of high strength steel fibre reinforced concrete corbels", *Compos. Struct.*, **93**(9), 2277-2287. https://doi.org/10.1016/j.compstruct.2011.03.016.

Abualnour, M., Chikh, A., Hebali, H., Kaci, A., Tounsi, A., Bousahla, A.A. and Tounsi, A. (2019), "Thermomechanical analysis of antisymmetric laminated reinforced composite plates using a new four variable trigonometric refined plate theory", *Comput. Concrete, Int. J.*, **24**(6), 489-498. https://doi.org/10.12989/cac.2019.24.6.489.

Addou, F.Y., Meradjah, M., Bousahla, A.A., Benachour, A., Bourada, F., Tounsi, A. and Mahmoud, S.R. (2019), "Influences of porosity on dynamic response of FG plates resting on Winkler/Pasternak/Kerr foundation using quasi 3D HSDT", *Comput. Concrete, Int. J.*, **24**(4), 347-367. https://doi.org/10.12989/cac.2019.24.4.347.

Alabduljabbar, H., Haido, J.H., Alyousef, R., Yousif, S.T., McConnell, J., Wakil, K. and Jermsittiparsert, K. (2020), "Prediction of the flexural behavior of corroded concrete beams using combined method", *Structures*, **25**, 1000-1008. https://doi.org/10.1016/j.istruc.2020.03.057.

Ali, A., Rajakumar, C. and Yunus, S.M. (1995), "Advances in acoustic eigenvalue analysis using boundary element method", *Comput. Struct.*, **56**(5), 837-847. https://doi.org/10.1016/0045-7949(95)00012-6.

Alimirzaei, S., Mohammadimehr, M. and Tounsi, A. (2019), "Nonlinear analysis of viscoelastic micro-composite beam with geometrical imperfection using FEM: MSGT electro-magneto-elastic bending, buckling and vibration solutions", *Struct. Eng. Mech., Int. J.*, **71**(5), 485-502. https://doi.org/10.12989/sem.2019.71.5.485.

Anbukarasi, K. and Kalaiselvam, S. (2015), "Study of effect of fibre volume and dimension on mechanical, thermal, and water absorption behaviour of luffa reinforced epoxy composites", *Mater. Des.*, **66**, 321-330. https://doi.org/10.1016/j.matdes.2014.10.078.

Arrakhiz, F.Z., Achaby, M.E.I., Malha, M., Bensalah, M.O., Fassi-Fehri, O., Bouhfid R., Benmoussa, K. and Qaiss, A. (2013), "Mechanical and thermal properties of natural fibres reinforced polymer composites: Doum/low density polyethylene", *Mater. Des.*, **43**, 200-205. https://doi.org/10.1016/j.matdes.2012.06.056.

Astley, R.J. (1985), "A finite element, wave envelope formulation for acoustical radiation in moving flows", *J. Sound Vib.*, **103**(4), 471-485. https://doi.org/10.1016/S0022-460X(85)80016-X.

Atalla, N. and Sgard, F. (2015), *Finite Element and Boundary Methods in Structural, Acoustics and Vibration*, CRC Press, New York, USA. https://doi.org/10.1201/b18366.

Atalla, N., Nicolas, J. and Gauthier, C. (1996), "Acoustic radiation of an unbaffled vibrating plate with general elastic boundary conditions", *J. Acoust. Soc. Am.*, **99**(3), 1484-1494. https://doi.org/10.1121/1.414727.

Balubaid, M., Tounsi, A., Dakhel, B. and Mahmoud, S.R. (2019), "Free vibration investigation of FG nanoscale plate using nonlocal two variables integral refined plate theory", *Comput. Concrete, Int. J.*, **24**(6), 579-586. https://doi.org/10.12989/cac.2019.24.6.579.

Béakou, A., Ntenga, R., Lepetit, J., Atéba, J.A. and Ayina, L.O. (2008), "Physico-chemical and microstructural characterization of Rhectophyllum camerunense plant fibre", *Compos. Part A Appl. Sci. Manuf.*, **39**(1), 67-74. https://doi.org/10.1016/j.compositesa.2007.09.002.

Belaadi, A., Bezazi, A., Bourchak, M. and Scarpa, F. (2013), "Tensile static and fatigue behaviour of sisal fibres", *Mater. Des.*, **46**, 76-83. https://doi.org/10.1016/j.matdes.2012.09.048.

Belbachir, N., Draich, K., Bousahla, A.A., Bourada, M., Tounsi, A. and Mohammadimehr, M. (2019), "Bending analysis of anti-symmetric cross-ply laminated plates under nonlinear thermal and mechanical loadings", *Steel Compos. Struct., Int. J.*, **33**(1), 81-92. https://doi.org/10.12989/scs.2019.33.1.081.

Berardi, U. and Iannace, G. (2015), "Acoustic characterization of natural fibres for sound absorption applications", *Build. Environ.*, **94**(2), 840-852. https://doi.org/10.1016/j.buildenv.2015.05.029.

Bert, C.W. and Malik, M. (1995), "Free vibration characteristics of symmetric cross-ply laminated plates: A semi-analytical differential quadrature analysis", *Comput. Mech.*, **95**, 2514-2519. https://doi.org/10.1007/978-3-642-79654-8_417.

Bousahla, A.A., Bourada, F., Mahmoud, S.R., Tounsi, A., Algarni, A., Bedia, E.A. and Tounsi, A. (2020), "Buckling and dynamic behavior of the simply supported CNT-RC beams using an integral-first shear deformation theory", *Comput. Concrete, Int. J.*, **25**(2), 155-166. https://doi.org/10.12989/cac.2020.25.2.155.

Boussoula, A., Boucham, B., Bourada, M., Bourada, F., Tounsi, A., Bousahla, A.A. and Tounsi, A. (2020), "A simple nth-order shear deformation theory for thermomechanical bending analysis of different configurations of FG sandwich plates", *Smart Struct. Syst., Int. J.*, **25**(2), 197-218. https://doi.org/10.12989/sss.2020.25.2.197.

Boutaleb, S., Benrahou, K.H., Bakora, A., Algarni, A., Bousahla, A.A., Tounsi, A., Tounsi, A. and Mahmoud, S. (2019), "Dynamic analysis of nanosize FG rectangular plates based on simple nonlocal quasi 3D HSDT", *Adv. Nano Res., Int. J.*, **7**(3), 191-208. https://doi.org/10.12989/anr.2019.7.3.191.

Cook, R.D., Malkus, D.S. and Plesha, M.E. (2000), *Concepts and Applications of Finite Element Analysis*, John Willy and Sons,

Singapore.

Dayo, A.Q., Gao, B.C., Wang, J., Liu, W.B., Derradji, M., Shah, A.H. and Babar, A.A. (2017), "Natural hemp fibre reinforced polybenzoxazine composites: curing behavior, mechanical and thermal properties", *Compos. Sci. Technol.*, **144**, 114-124. https://doi.org/10.1016/j.compscitech.2017.03.024.

Demir, H., Atikler, U., Balkose, D. and Tıhmınlıoglu, F. (2006), "The effect of fibre surface treatments on the tensile and water sorption properties of polypropylene – luffa fibre composites", *Compos. Part A Appl. Sci. Manuf.*, **37**(3), 447-456. https://doi.org/10.1016/j.compositesa.2005.05.036.

Draiche, K., Bousahla, A.A., Tounsi, A., Alwabli, A.S., Tounsi, A. and Mahmoud, S.R. (2019), "Static analysis of laminated reinforced composite plates using a simple first-order shear deformation theory", *Comput. Concrete, Int. J.*, **24**(4), 369-378. https://doi.org/10.12989/cac.2019.24.4.369.

Draoui, A., Zidour, M., Tounsi, A. and Adim, B. (2019), "Static and dynamic behavior of nanotubes-reinforced sandwich plates using FSDT", *J. Nano Res.*, **57**, 117-135. https://doi.org/10.4028/www.scientific.net/JNanoR.57.117.

Erosy, S. and Kucuk, H. (2009), "Investigation of industrial tea-leaf waste material for its sound absorption properties", *Appl. Acoust.*, **70**, 215-220. https://doi.org/10.1016/j.apacoust.2007.12.005.

Everstine, G.C. and Henderson, F.M. (1990), "Coupled finite element/boundary element approach for fluid-structure interaction", *J. Acoust. Soc. India*, **87**(5), 1938-1947. https://doi.org/10.1121/1.399320.

Ganapathi, M. and Kalyani, A., Mondal, B. and Prakash, T. (2009), "Free vibration analysis of simply supported composite laminated panels", *Compos. Struct.*, **90**(1), 100-103. https://doi.org/10.1016/j.compstruct.2009.02.003.

Gibson, R.F. (2000), "Modal vibration response measurements for characterization of composite materials and structures", *Compos. Sci. Technol.*, **60**(15), 2769-2780. https://doi.org/10.1016/S0266-3538(00)00092-0.

Haido, J.H. (2020), "Flexural behavior of basalt fiber reinforced concrete beams: Finite element simulation with new constitutive relationships", *Structures*, **27**, 1876-1889. https://doi.org/10.1016/j.istruc.2020.08.005.

Hosseini Fouladi, M., Jailani, M.N.M., Ayub, M. and Leman, Z.A. (2010), "Utilization of coir fibre in multilayer acoustic absorption panel", *Appl. Acoust.*, **71**(3), 241-249. https://doi.org/10.1016/j.apacoust.2009.09.003.

Jayamani, E., Hamdan, S., Rahman, M.R., Heng, S.K. and Bin Bakri, M.K. (2014), "Processing and characterization of Epoxy/Luffa Composites: Investigation on chemical treatment of fibres on mechanical and acoustical properties", *Acoust. Absorb.*, **9**(3), 5542-5556.

Jayamani, E., Hamdan, S., Bakri Bin, M.K., Soon Kok, H., Rahman, M.R. and Kakar, A. (2016), "Analysis of natural fibre polymer composites: Effects of alkaline treatment on sound absorption", *J. Reinf. Plast. Compos.*, **35**(9), 703-711. https://doi.org/10.1177/0731684415620046.

Jeyaraj, P. (2010), "Vibroacoustic behavior of an isotropic plate with arbitrarily varying thickness", *Eur. J. Mech A/Solids*, **29**(6), 1088-1094. https://doi.org/10.1016/j.euromechsol.2010.05.009.

Joshi, S.V., Drzal, L.T., Mohanty, A.K. and Arora, S. (2004), "Are natural fibre composites environmentally superior to glass fibre reinforced composites?", *Compos. Part A Appl. Sci. Manuf.*, **35**(3), 371-376. https://doi.org/10.1016/j.compositesa.2003.09.016.

Junge, M., Brunner, D. and Gaul, L. (2011), "Solution of FE-BE coupled eigenvalue problems for the prediction of the vibroacoustic behavior of ship-like structures", *Int. J. Numer. Methods Eng.*, **87**, 664-676. https://doi.org/10.1002/nme.3124.

Kaddari, M., Kaci, A., Bousahla, A.A., Tounsi, A., Bourada, F., Tounsi, A., Bedia, E.A. and Al-Osta, M. (2020), "A study on the structural behaviour of functionally graded porous plates on elastic foundation using a new quasi-3D model: Bending and free vibration analysis", *Comput. Concrete, Int. J.*, **25**(1), 37-57. https://doi.org/10.12989/cac.2020.25.1.037.

Kant, T. and Swaminathan, K. (2001), "Free vibration of isotropic, orthotropic, and multilayer plates based on higher order refined theories", *J. Sound Vib.*, **241**(2), 319-327. https://doi.org/10.1006/jsvi.2000.3232

Karami, B., Janghorban, M. and Tounsi, A. (2019a), "Galerkin's approach for buckling analysis of functionally graded anisotropic nanoplates/different boundary conditions", *Eng. Comput., Int. J.*, **35**, 1297-1316. https://doi.org/10.1007/s00366-018-0664-9.

Karami, B., Shahsavari, D., Janghorban, M. and Tounsi, A. (2019b), "Resonance behavior of functionally graded polymer composite nanoplates reinforced with graphene nanoplatelets", *Int. J. Mech. Sci.*, **156**, 94-105. https://doi.org/10.1016/j.ijmecsci.2019.03.036.

Karami, B., Janghorban, M. and Tounsi, A. (2020), "Novel study on functionally graded anisotropic doubly curved nanoshells", *Eur. Phys. J. Plus*, **135**(1), 103. https://doi.org/10.1140/epjp/s13360-019-00079-y.

Khdeir, A.A. and Reddy, J.N. (1999), "Free vibrations of laminated composite plates using second-order shear deformation theory", *Comput. Struct.*, **71**(6), 617-626. https://doi.org/10.1016/S0045-7949(98)00301-0.

Khiloun, M., Bousahla, A.A., Kaci, A., Bessaim, A., Tounsi, A. and Mahmoud, S.R. (2020), "Analytical modeling of bending and vibration of thick advanced composite plates using a four-variable quasi 3D HSDT", *Eng. Comput.*, **36**(3), 807-821. https://doi.org/10.1007/s00366-019-00732-1.

Khosravi, F., Hosseini, S.A. and Tounsi, A. (2020), "Torsional dynamic response of viscoelastic SWCNT subjected to linear and harmonic torques with general boundary conditions via Eringen's nonlocal differential model", *Eur. Phys. J. Plus*, **135**(2), 183. https://doi.org/10.1140/epjp/s13360-020-00207-z.

Kong, Q., He, X., Shu, L. and Miao, M.S. (2017), "Ofloxacin adsorption by activated carbon derived from luffa sponge: Kinetic, isotherm, and thermodynamic analyses", *Process Saf. Environ. Prot.*, **112**, 254-264. https://doi.org/10.1016/j.psep.2017.05.011.

Koruk, H. and Genc, G. (2015), "Investigation of the acoustic properties of bio luffa fibre and composite materials", *Mater. Lett.*, **157**, 166-168. https://doi.org/10.1016/j.matlet.2015.05.071.

Küçük, M. and Korkmaz, Y. (2012), "The effect of physical parameters on sound absorption properties of natural fibre mixed nonwoven composites", *Text. Res. J.*, **82**(20), 2043-2053. https://doi.org/10.1177/0040517512441987.

Kumar, B.R., Ganesan, N. and Sethuraman, R. (2010), "Vibroacoustic analysis of composite elliptic disc with various orthotropic properties", *J. Compos. Mater.*, **44**(10), 1179-1200. https://doi.org/10.1177/0021998309349016.

Kumar, K.S., Siva, I., Jeyaraj, P., Jappes, J.T.W., Amico, S.C. and Rajini, N. (2014), "Synergy of fibre length and content on free vibration and damping behavior of natural fibre reinforced polyester composite beams", *Mater. Des.*, **56**, 379-386. https://doi.org/10.1016/j.matdes.2013.11.039.

Li, S. and Li, X. (2008), "The effects of distributed masses on acoustic radiation behavior of plates", *Appl. Acoust.*, **69**(3), 272-279. https://doi.org/10.1016/j.apacoust.2006.11.004.

Liew, K.M. (2003), "Vibration analysis of symmetrically laminated plates based on FSDT using the moving least squares differential quadrature method", *Comput. Methods Appl. Mech. Eng.*, **192**(19), 2203-2222. https://doi.org/10.1016/S0045-7825(03)00238-X.

Medani, M., Benahmed, A., Zidour, M., Heireche, H., Tounsi, A.,

Bousahla, A.A., Tounsi, A. and Mahmoud, S.R. (2019), "Static and dynamic behavior of (FG-CNT) reinforced porous sandwich plate using energy principle", *Steel Compos. Struct., Int. J.*, **32**(5), 595-610. https://doi.org/10.12989/scs.2019.32.5.595.

Meyer, W.L., Bell, W.A., Zinn, B.T. and Stallybrass, M.P. (1978), "Boundary integral solutions of three dimensional acoustic radiation problems", *J. Sound Vib.*, **59**(2), 245-262. https://doi.org/10.1016/0022-460X(78)90504-7.

Rajesh, M. and Pitchaimani, J. (2017), "Experimental investigation on buckling and free vibration behavior of woven natural fibre fabric composite under axial compression" *Compos. Struct.*, **163**, 302-311. https://doi.org/10.1016/j.compstruct.2016.12.046.

Nowak, L.J. and Zielinski, T.G. (2015), "Determination of the free-field acoustic radiation characteristics of the vibrating plate structures with arbitrary boundary conditions", *J. Vib. Acoust.*, **137**, 51001. https://doi.org/10.1115/1.4030214.

Ohlrich, M. and Hugin, C.T. (2004), "On the influence of boundary constraints and angled baffle arrangements on sound radiation from rectangular plates", *J. Sound Vib.*, **277**(1-2), 405-418. https://doi.org/10.1016/j.jsv.2003.11.038.

Park, J., Mongeau, L. and Siegmund, T. (2003), "Influence of support properties on the sound radiated from the vibrations of rectangular plates", *J. Sound Vib.*, **264**(4), 775-794. https://doi.org/10.1016/S0022-460X(02)01215-4.

Peters, H., Kessissoglou, N. and Marburg, S. (2014), "Modal decomposition of exterior acoustic-structure interaction", *J. Acoust. Soc. Am.*, **135**(5), 2668-2677. https://doi.org/10.1121/1.4796114.

Petrone, G., D'Alessandro, V., Franco, F. and De Rosa, S. (2014), "Numerical and experimental investigations on the acoustic power radiated by aluminium foam sandwich panels", *Compos. Struct.*, **118**, 170-177. https://doi.org/10.1016/j.compstruct.2014.07.031.

Prabhakaran, S., Krishnaraj, V., Kumar, M.S. and Zitoune, R. (2014), "Sound and vibration damping of flax fibre reinforced composites", *Procedia Eng.*, **97**, 573-581. https://doi.org/10.1016/j.proeng.2014.12.285.

Putra, A. and Thompson, D.J. (2010), "Sound radiation from rectangular baffled and unbaffled plates", *Appl. Acoust.*, **71**(12), 1113-1125. https://doi.org/10.1016/j.apacoust.2010.06.009.

Putra, A., Abdullah, Y., Efendy, H., Farid, W.M., Ayob, M.R. and Py, S.M. (2013), "Utilizing sugarcane wasted fibres as a sustainable acoustic absorber", *Proceedings of Malaysian University Confrence on Engineering and Technology Part 2-Mechanical and Manufacturing Engineering*, Hang Tuah Jaya, Malaysia, September.

Rajini, N., Jappes, J.W., Rajakarunakaran, S. and Jeyaraj, P. (2013), "Dynamic mechanical analysis and free vibration behavior in chemical modifications of coconut sheath/nano-clay reinforced hybrid polyester composite", *J. Compos. Mater.*, **47**(24), 3105-3121. https://doi.org/10.1177/0021998312462618.

Sahla, M., Saidi, H., Draiche, K., Bousahla, A.A., Bourada, F. and Tounsi, A. (2019), "Free vibration analysis of angle-ply laminated composite and soft core sandwich plates", *Steel Compos. Struct., Int. J.*, **33**(5), 663-679. https://doi.org/https://doi.org/10.12989/scs.2019.33.5.663.

Seddeq, H.S., Aly, M.N., Marwa A.A. and Elshakankery, M.H. (2012), "Investigation on sound absorption properties for recycled fibrous materials", *J. Ind. Text.*, **43**(1), 56-73. https://doi.org/10.1177/1528083712446956.

Senthilkumar, K., Saba, N., Chandrasekar, M., Jawaid, M., Rajini, N., Alothman, O.Y. and Siengchin, S. (2019), "Evaluation of mechanical and free vibration properties of the pineapple leaf fibre reinforced polyester composites", *Constr. Build. Mater.*, **195**, 423-431. https://doi.org/10.1016/j.conbuildmat.2018.11.081.

Sgriccia, N., Hawley, M.C. and Misra, M. (2008), "Characterization of natural fibre surfaces and natural fibre composites", *Compos. Part A Appl. Sci. Manuf.*, **39**(10), 1632-1637. https://doi.org/10.1016/j.compositesa.2008.07.007.

Shariati, M., Mafipour, M.S., Haido, J.H., Yousif, S.T., Toghroli, A., Trung, N.T. and Shariati, A. (2020), "Identification of the most influencing parameters on the properties of corroded concrete beams using an adaptive neuro-fuzzy inference system (ANFIS)", *Steel Compos. Struct., Int. J.*, **34**(1), 155-170. https://doi.org/https://doi.org/10.12989/scs.2020.34.1.155.

Shen, J., Xie, Y.M., Huang, X., Zhou, S. and Ruan, D. (2012), "Mechanical properties of luffa sponge", *J. Mech. Behav. Biomed. Mater.*, **15**, 141-152. https://doi.org/10.1016/j.jmbbm.2012.07.004.

Shen, J., Xie, Y.M., Huang, X., Zhou, S. and Ruan, D. (2013), "Behaviour of luffa sponge material under dynamic loading", *Int. J. Impact Eng.*, **57**, 17-26. https://doi.org/10.1016/j.ijimpeng.2013.01.004.

Tounsi, A., Al-Dulaijan, S.U., Al-Osta, M.A., Chikh, A., Al-Zahrani, M.M., Sharif, A. and Tounsi, A. (2020), "A four variable trigonometric integral plate theory for hygro-thermo-mechanical bending analysis of AFG ceramic-metal plates resting on a two-parameter elastic foundation", *Steel Compos. Struct., Int. J.*, **34**(4), 511-524. http://dx.doi.org/10.12989/scs.2020.34.4.511.

Tournour, M. and Atalla, N. (1998), "Vibroacoustic behavior of an elastic box using state-of-the-art FEM-BEM approaches", *Noise Control Eng. J.*, **46**(3), 83-90. https://doi.org/10.3397/1.2828460.

Wang, K.F. and Wang, B.L. (2018), "A mechanical degradation model for bidirectional natural fibre reinforced composites under hydrothermal ageing and applying in buckling and vibration analysis", *Compos. Struct.*, **206**, 594-600. https://doi.org/10.1016/j.compstruct.2018.08.063.

Wielage, B., Lampke, T., Utschick, H. and Soergel, F. (2003), "Processing of natural-fibre reinforced polymers and the resulting dynamic-mechanical properties", *J. Mater. Process. Technol.*, **139**(1-3), 140-146. https://doi.org/10.1016/S0924-0136(03)00195-X.

Xu, C., Zhang, X., Haido, J.H., Mehrabi, P., Shariati, A., Mohamad, E.T., Hoang, N. and Wakil, K. (2019), "Using genetic algorithms method for the paramount design of reinforced concrete structures", *Struct. Eng. Mech., Int. J.*, **71**(5), 503-513. https://doi.org/10.12989/sem.2019.71.5.503.

Yin, X.W. and Cui, H.F. (2009), "Acoustic radiation from a laminated composite plate excited by longitudinal and transverse mechanical drives", *J. Appl. Mech.*, **76**(4), 44501-44505. https://doi.org/10.1115/1.3086429.

CC